

## Article

# Degradation of STK16 via KCTD17 with Ubiquitin–Proteasome System in Relation to Sleep–Wake Cycle

Susumu Tanaka <sup>1,\*</sup> , Yoshiko Honda <sup>2</sup>, Misa Sawachika <sup>1</sup>, Kensuke Futani <sup>1</sup>, Namika Yoshida <sup>1</sup> and Tohru Kodama <sup>2</sup>

<sup>1</sup> Department of Nutrition Science, Faculty of Nursing and Nutrition, University of Nagasaki, Siebold, 1-1-1 Manabino, Nagayo-cho, Nishi-Sonogi-gun, Nagasaki 851-2195, Japan

<sup>2</sup> SLEEP Disorders Project, Tokyo Metropolitan Institute of Medical Science, Tokyo 156-8506, Japan

\* Correspondence: tanakass@sun.ac.jp; Tel.: +81-95-813-5212

**Abstract:** Serine/threonine-protein kinase 16 (STK16) is a novel member of the Numb-associated family of protein kinases with an atypical kinase domain. In this study, we aimed to investigate the involvement of STK16 in sleep–wake mechanisms. We confirmed the expression of *Stk16* in the murine hypothalamus, the sleep–wake center, and found considerable changes in STK16 protein levels in the anterior hypothalamus during the light–dark cycle. We found that the coexistence of the potassium channel tetramerization domain containing 17 (KCTD17), an STK16 interactor, caused STK16 degradation. In contrast, the proteasome inhibitor MG132 inhibited the degradation of STK16. In addition, polyubiquitinated STK16 was observed, suggesting that KCTD17 acts as an adapter for E3 ligase to recognize STK16 as a substrate, leading to STK16 degradation via the ubiquitin–proteasome system. The vast changes in STK16 in the anterior hypothalamus, a mammalian sleep center, as well as the reported sleep abnormalities in the ubiquitin B knockout mice and the *Drosophila* with the inhibition of the KCTD17 homolog or its E3 ligase cullin-3, suggest that STK16 plays a major role in sleep–wake regulation.

**Keywords:** STK16; KCTD17; ubiquitin; proteasome; hypothalamus; sleep



**Citation:** Tanaka, S.; Honda, Y.; Sawachika, M.; Futani, K.; Yoshida, N.; Kodama, T. Degradation of STK16 via KCTD17 with Ubiquitin–Proteasome System in Relation to Sleep–Wake Cycle. *Kinases Phosphatases* **2023**, *1*, 14–22. <https://doi.org/10.3390/kinasesphosphatases1010003>

Academic Editor: Mauro Salvi

Received: 25 November 2022

Revised: 9 December 2022

Accepted: 12 December 2022

Published: 22 December 2022



**Copyright:** © 2022 by the authors. Licensee MDPI, Basel, Switzerland. This article is an open access article distributed under the terms and conditions of the Creative Commons Attribution (CC BY) license (<https://creativecommons.org/licenses/by/4.0/>).

## 1. Introduction

Serine/threonine-protein kinases (STKs) are enzymes that phosphorylate the OH group of serine or threonine, two amino acids with similar side chains. Among all the protein kinases identified in humans, at least 350 are STKs [1]. STK16 was first identified as a protein kinase expressed in day 12 fetal liver (PKL12) [2]. Since STK16 is conserved among vertebrates, the discovery process was diverse, and included kinases related to *Saccharomyces cerevisiae* and *Arabidopsis thaliana* [3], embryo-derived protein kinase [4], myristoylated and palmitoylated Ser/Thr protein kinase [5], and transforming growth factor (TGF)- $\beta$ -1 [6]. STK16 is ubiquitously expressed in several tissues during the developmental and adult stages [2,7]. STK16 is also expressed in a variety of cell lines; it mainly localizes to the Golgi apparatus [2,8–10] and translocates to the nucleus under certain circumstances [8]. STK16 is a novel member of the Numb-associated family of protein kinases (NAKs), with an atypical kinase structure and function [11,12]. The crystal structure of STK16 shows an atypical activation loop architecture in the catalytic domain known as the activation segment C terminal helix [12]. In vitro studies showed that STK16 is capable of autophosphorylation in addition to the phosphorylation of various substrates [7]. Recent studies have revealed that STK16 plays critical roles in the cell cycle, intracellular signaling, Golgi assembly, and sorting and secretion of proteins via phosphorylation; however, it is still a relatively poorly understood kinase [7].

In the brain, the changes in the “percent spliced in” [13] of STK16 are associated with the expression changes of the ETS transcription factor ELK1, which is closely related to

low-grade glioma and its target genes [14]. N-acetylglucosamine kinase (NAGK) is an established interactor of STK16 [9] that is highly expressed in neurons [15]. In neurons, the interaction between N-acetylglucosamine (GlcNAc), dynein, and Golgi can regulate the growth of axons [16] and dendrites [17]. NAGK is involved in the hexosamine biosynthesis pathway, a well-known glucose metabolic pathway, and its metabolites, uridine diphosphate (UDP)-N-acetyl-glucosamine, N-acetylneuraminic acid, N-acetyl-d-mannosamine, and sialic acid [18,19] have been implicated in hypocretin/orexin neuron differentiation [20–22]. Hypocretins are neuropeptides produced in the posterior hypothalamus, and are involved in the regulation of the sleep–wake cycle [23,24]. It is well known that the sleep/wake state transitions are based on mutual inhibitory circuits between the anterior and posterior hypothalamic areas, as observed in electronic flip-flop switches [25]. Therefore, in this study, to understand the involvement of STK16 in the sleep–wake cycle, we confirmed the expression of *STK16* in the murine anterior and posterior hypothalamus, and unexpectedly found considerable changes in *STK16* expression during the light–dark cycle in the anterior hypothalamus. Furthermore, we observed an increase in the STK16 protein levels in the light phase, as well as its disappearance in the dark phase of the anterior hypothalamus. In addition, we examined whether this decrease was mediated by the proteolytic pathway.

## 2. Results

*STK16* expression in the murine anterior hypothalamus was decreased in the dark phase compared to that in the light phase ( $p < 0.05$ , Figure 1A). In contrast, no significant difference was observed between the light and dark phases in the murine posterior hypothalamus. STK16 protein levels were detectable at ZT0, peaked at ZT6, and dropped below the detection limit during the dark phase (ZT12 and ZT18) (Figure 1B). Since this sharp decrease suggested the involvement of proteolytic pathways, we explored their possible involvement in STK16 degradation using the BioGRID database, a biomedical interaction repository [26]. One possible protein, the potassium channel tetramerization domain containing 17 (KCTD17), which interacts with the cullin E3 (CUL3) ubiquitin ligase complex [27] involved in the ubiquitin–proteasome pathway [28], was identified in the BIOGRID database. There were no significant changes in the level of KCTD17 protein, predicted at 50 kDa and 40 kDa in the light and dark cycle; however, short isoforms, which were predicted to weight around 30 kDa, were significantly increased in the light phase. This suggests that KCTD17 may have undergone limited light-phase-specific degradation (Figure 1B arrowhead, Figure S1).

We next examined whether KCTD17 was involved in the degradation of STK16. HEK293T cells were transfected with the STK16-HA and KCTD17-FLAG vectors. Endogenous CUL3 was detected in HEK293T cells, and the coexistence of KCTD17 confirmed a significant loss of STK16 (Figures 2 and S2). In the preliminary study, we found that the STK16-myc fusion was difficult to degrade; therefore, we examined whether STK16 and KCTD17 bound directly to each other using STK16-myc. The anti-myc antibody co-immunoprecipitated STK16-myc with KCTD17-FLAG, and the anti-FLAG antibody co-immunoprecipitated STK16-myc with KCTD17-FLAG (Figure 2B).

Finally, inhibition experiments with a potent non-specific 20S proteasome inhibitor, MG132 [29], were performed to confirm that STK16 degradation was mediated by the proteasome system. MG132 significantly inhibited the degradation of STK16 by KCTD17. Moreover, since ubiquitin weighs 7 kDa, we could smoothly detect the bands every 7 kDa, which were considered to form the polyubiquitinated STK16 ladder. These polyubiquitinated STK16s would normally be translocated and degraded by the ubiquitin–proteasome system (Figures 3 and S3).

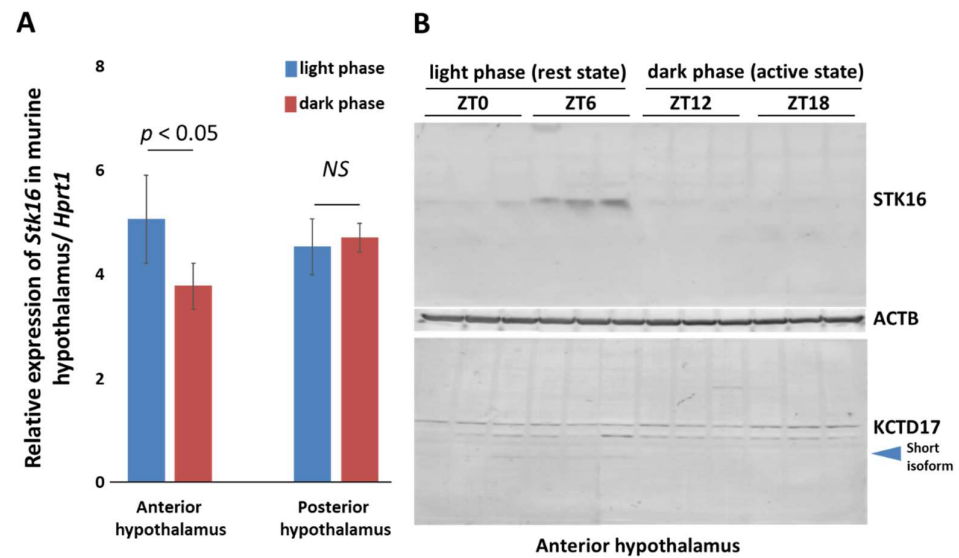


**Figure 1.** Diurnal changes in STK16. **(A)** The relative expression levels of *Stk16* in murine hypothalamus were evaluated by using the  $2^{-\Delta\Delta Cq}$  method, with hypoxanthine phosphoribosyltransferase 1 (*Hprt1*) as an internal control. *Stk16* expression was significantly decreased in the dark phases of the anterior hypothalamus compared with the light phases. **(B)** STK16 protein levels were considerably decreased in the dark phases of the anterior hypothalamus. Short isoforms of KCTD17 were only detected in the light phases. NS: Not significant.

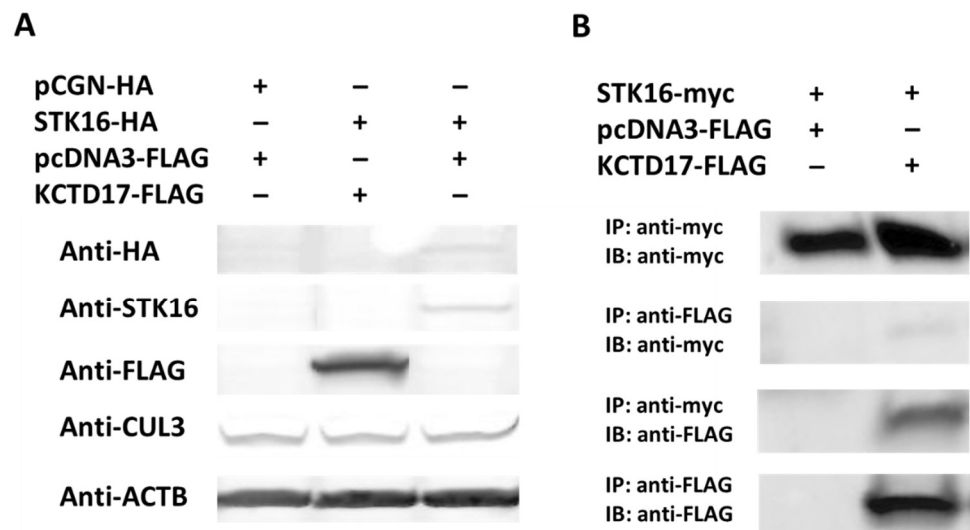


**Figure 2.** STK16 was degraded in the presence of KCTD17. **(A)** Co-transfection of STK16-HA and KCTD17-FLAG expression vectors into HEK293T cells induced STK16-HA degradation. **(B)** STK16-myc and KCTD17-FLAG proteins were co-immunoprecipitated.

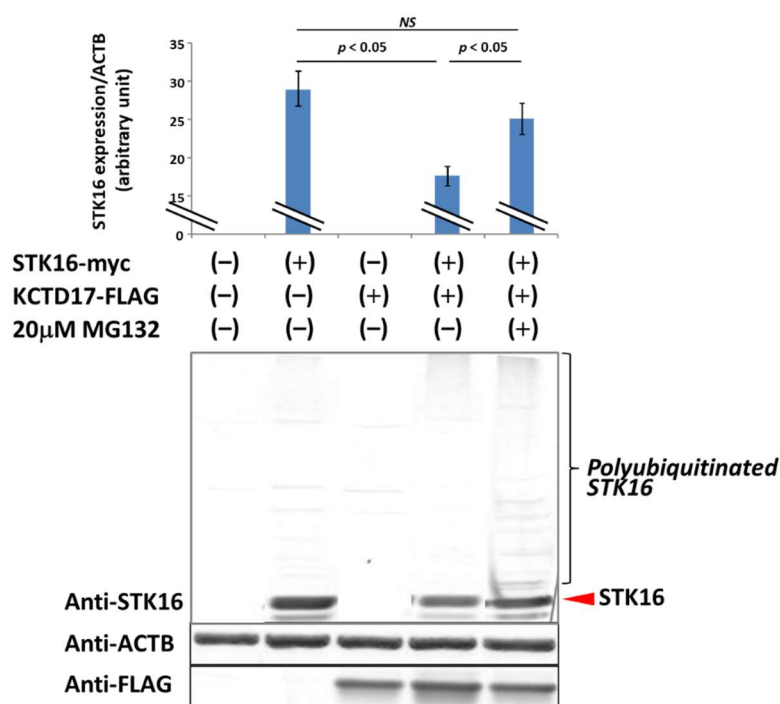


**Figure 3.** Inhibition of STK16 degradation by the proteasome inhibitor MG132. MG132 (20  $\mu$ M) inhibited the degradation of STK16 by KCTD17. Inhibition of the proteasome system by MG132 allowed for the detection of the polyubiquitinated STK16. NS: Not significant.

### 3. Discussion

In this study, we found rapid changes in STK16 levels during the light-dark cycle in the anterior hypothalamus, which may have been mediated by the KCTD17-mediated ubiquitin–proteasome system. It was also suggested that the rapid degradation of STK16 protein in the anterior hypothalamus, known as the sleep center, may play an important role in the sleep–wake transition. Ubiquitin is a highly conserved polypeptide of 76 amino acids that is ubiquitous in the eukaryotic kingdom [30]. Ubiquitin binds covalently to substrates, often forming polymers, by a process known as the polyubiquitination of the substrate. Its main function is the transport of substrates to the proteasome, a multi-subunit protease, for degradation [30]. Although the mechanisms of ubiquitination reactions vary, these reactions usually occur with the help of a series of enzymes, including an activating enzyme (E1), a binding enzyme (E2), and a ligase (E3). In the presence of the E3 ligase and an adapter with substrate specificity, ubiquitin molecules are attached to the substrate [31,32]. In the present study, we identified CUL3 as a potential E3 ligase and KCTD17 as an adapter to recognize STK16 as a substrate. When MG132, a proteasome inhibitor, was added in the presence of KCTD17, a band of STK16 was detected every 7 kDa. This indicates that polyubiquitinated chains of various lengths are bound to STK16, which are assumed to be involved in the transport of STK16 to the proteasome and its subsequent degradation. In the murine brain sample, a significant change in the levels of KCTD17 short isoforms during the sleep–wake cycle was observed. KCTD17 is known to bind to other family proteins [33] and also to interact with itself [34]. Therefore, the 50, 40, and 30 kDa isoforms are likely to interact with each other. Furthermore, it is necessary to identify the amino acid sequence of each isoform from brain samples and study the differences in STK16 degradation in vitro by the corresponding generated recombinant proteins in the future. On the other hand, the importance of the unstructured region in substrate recognition in the proteasome has been suggested, and the nature of the unstructured region is known to be a determining factor in the subunit-specific degradation of protein complexes [35]. In addition, it has been reported that protein binding to the unstructured region suppresses protein degradation, and it is predicted that many more proteins are regulated through

the unstructured region [36]. Therefore, it is possible that differences in STK16 substrate recognition may be caused by differences in the unstructured region of KCTD17, due to isoform differences.

A forward genetic study on *Drosophila* identified a mutation in *insomniac* (*inc*), a gene associated with insomnia [37–39]. Restricted *inc* expression with *pars intercerebralis*, a counterpart of the mammalian hypothalamus–pituitary structure, driver in a mutant, indicated behavioral rescue. The *insomniac* protein is a homolog of KCTD17 [39], which interacts with the CUL3 E3 ubiquitin ligase complex [39]. The RNAi-mediated knockdown of CUL 3 caused a decrease in sleep duration, suggesting that the ubiquitin–proteasome pathway regulates sleep/wakefulness in *Drosophila*. In addition, the polyubiquitin gene (*Ubb*) knockout mice showed unusual metabolic rates and sleep homeostasis, suggesting that *Ubb* is essential for the maintenance of the ubiquitin levels required for the proper regulation of metabolic and sleep behaviors [40]. Future sleep analysis in STK16 knockout mice is needed, as the *Ubb* knockout may have caused a derangement in STK16 regulation, resulting in sleep abnormalities.

Sustained wakefulness results in the accumulation of sleep-promoting somatic factors, including adenosine, subsequently causing an increase in sleep pressure or parasomnias [41]. Adenosine is an endogenous sleep regulator that activates the anterior hypothalamus via the adenosine A1 and A2A receptors to promote sleep [42]. Although there are other known substances similar to adenosine, in that they accumulate during sustained wakefulness and induce sleep, only a few are known to increase during sleep and disappear upon awakening, such as STK16, which was discovered in this study. STK16 may be an endogenous modulator that indicates sleep duration to be sufficient and also promotes brain arousal. Increasing sleep pressure via sleep deprivation manipulation does not cause changes if the former is a rhythm factor, as rhythm factors take time to synchronize, as is known for jet lag [43,44]; sleep deprivation experiments may facilitate the identification of STK16 as a sleep–wake modulator. In contrast, 80 proteins were identified, phosphorylation states of which are closely related to changes in sleep desire, and most of which are closely related to synapses [45]. Furthermore, sleep induction via CaMKII, an enzyme important for synaptic plasticity [46], has also been reported [47]. Therefore, we speculate that STK16 may be involved in these synaptic regulatory mechanisms. Interaction between STK16 and synaptogyrin-2, a synapse-associated protein, has been previously reported [48]. Therefore, future studies are warranted to identify the STK16-expressing cells and study the subcellular localization of STK16 in the brain.

## 4. Materials and Methods

### 4.1. Animals

A total of 24 male C57BL/6J mice were obtained from Shimizu Laboratory Supplies Co., Ltd. (Kyoto, Japan) and housed under a 12-h light/dark cycle, with the lights on between 8:00 A.M. and 8:00 P.M., corresponding to zeitgeber time (ZT) 0–12. The temperature was maintained at 22–24 °C, and the mice were provided with food and water ad libitum. Twenty mice (weight, 28–30 g; age, 12 weeks) were sacrificed at ZT0, ZT6, ZT12, and ZT18 for analysis of mRNA expression and protein levels.

### 4.2. Quantitative PCR (qPCR)

Mice were deeply anesthetized with pentobarbital (50 mg/kg, i.p.), and whole brains were removed. The hypothalamic region was dissected coronally from the optic chiasma to the mammillary bodies (6 mm from the chiasma) using a brain slicer (Zivic Instruments; Pittsburgh, PA, USA). The anterior hypothalamus was defined as the area up to 3 mm from the chiasma. The distinction between the anterior and posterior hypothalami was based on the presence or absence of hypocretin expression. The dorsal limit of the hypothalamus was the roof of the third ventricle, and the lateral limit was the amygdala [49–52]. Total RNA was isolated from each region of the hypothalamus using the Sepasol-RNA I Super G reagent (Nacalai Tesque, Inc.; Kyoto, Japan). Single-stranded cDNA was synthesized using the

PrimeScript RT Reagent Kit with gDNA Eraser (Takara Bio, Inc.; Otsu, Japan), according to the manufacturer's protocol. The expression level of each mRNA was determined by qPCR using the Rotor-Gene Q system (Qiagen GmbH; Hilden, Germany), THUNDERBIRD™ qPCR mix (Toyobo Co., Ltd.; Osaka, Japan), as well as gene-specific primers (Table S1). PCR products were amplified using the following thermocycling conditions: one cycle at 95 °C for 1 min, followed by 40 cycles at 95 °C for 10 s and 60 °C for 60 s. The housekeeping gene with minimum diurnal variation in the hypothalamus was identified in a previous study by checking gene expression every 4 h over a 24-h period [50,53]. Subsequently, the relative level of target gene expression was evaluated using the 2- $\Delta\Delta C_q$  method, with hypoxanthine phosphoribosyltransferase 1 as an internal control.

#### 4.3. Expression Vectors and Cell Culture

Mouse *Stk16* and *Kctd17* cDNAs were amplified from the murine hypothalamus cDNA by PCR using KOD DNA polymerase (Toyobo Co., Ltd.), and subcloned into pCGN-HA (STK16-HA), pcDNA3.1-myc (STK16-myc), or pcDNA3-FLAG (KCTD17-FLAG). HEK293T cells (American Type Culture Collection; Manassas, VA, USA) were grown in Dulbecco's modified Eagle's medium (Gibco™; Thermo Fisher Scientific, Inc.; Waltham, MA, USA) supplemented with 10% fetal bovine serum (Gibco™; Thermo Fisher Scientific, Inc.) at 37 °C in an atmosphere containing 5% CO<sub>2</sub>. Cells were seeded at a density of  $3 \times 10^5$  cells/well in 6-well cell culture plates. Expression vectors were co-transfected into the HEK293 cells using Lipofectamine™ 3000 Transfection Reagent (Invitrogen; Thermo Fisher Scientific, Inc.; Waltham, MA, USA) according to the manufacturer's protocol. To inhibit the ubiquitin-proteasome pathway, 20  $\mu$ M of MG132 (Wako Pure Chemical Industries, Ltd.; Osaka, Japan), a potent non-specific 20S proteasome inhibitor, was added to the culture medium for 2 days after transfection.

#### 4.4. Immunoprecipitation

Approximately 48 h post-transfection, the transiently transfected cells were washed three times with ice-cold phosphate-buffered saline (PBS) before lysis with an immunoprecipitation (IP) buffer (20 mM Tris-HCl, 1 mM EDTA, 100 mM NaCl, pH 7.5, and 0.5% NP-40) containing the complete protease inhibitor cocktail (Roche Diagnostics; Tokyo, Japan). Subsequently, the cells were sonicated for 30 s, incubated for 15 min on ice, and centrifuged at  $12,000 \times g$  for 10 min at 4 °C. Next, the supernatant was incubated with an anti-myc [PL14] (MBL Co., Ltd.; Tokyo, Japan) or anti-FLAG antibody (Sigma-Aldrich; St. Louis, MO, USA). The tube was rotated overnight at 4 °C, followed by three washes with the IP buffer. The antibody-conjugated samples were immunoprecipitated using Protein G Sepharose (Roche Diagnostics).

#### 4.5. Immunoblotting Analysis

The murine hypothalamic tissues or HEK293T cells were homogenized using RIPA buffer (25 mM Tris-HCl pH 7.6, 150 mM NaCl, 1% NP-40, 1% sodium deoxycholate, 0.1% SDS) and the Protease Inhibitor Cocktail (Roche Diagnostics). The homogenate was then centrifuged, and the supernatant was obtained as a soluble fraction. An aliquot of 10  $\mu$ g of the soluble fraction of tissues or immunoprecipitated samples was electrophoresed through a denaturing gradient acrylamide gel, and then transferred to Clear Blot Membrane-P (ATTO; Tokyo, Japan). After blocking with 5% Blocking One (Nacalai Tesque, Inc.), the membranes were incubated with anti-FLAG (1:3000; Sigma-Aldrich), anti-myc (1:3000; MBL Co., Ltd.), anti-HA-561 (1:1000; MBL Co., Ltd.), anti-STK16 (H-80) (1:1000; Santa Cruz Biotechnology, Inc.; Dallas, TX, USA), anti-KCTD17 (1:1000; Abcam Inc.; Waltham, MA, USA), anti-Cullin 3 [EPR3196Y] (1:5000; Abcam Inc.), or monoclonal anti- $\beta$ -Actin [AC-15] (1:10,000; Sigma-Aldrich) antibody for 1 h at 20 °C and overnight at 4 °C. After washing three times for 10 min each with Tris-buffered saline (TBS) (150 mM NaCl, 20 mM Tris, pH 7.4)-0.05% Tween-20 (TBST), the membranes were incubated with a 1:5000 dilution of HRP-labeled protein-G (Merck Millipore; Burlington, MA, USA) in 1% Blocking One/TBST

for 1 h at 20 °C. Subsequently, the proteins were visualized using TMB Membrane Peroxidase Substrate (Kirkegaard & Perry Laboratories; Gaithersburg, MD, USA) and the reaction was stopped with tap water.

#### 4.6. Statistical Analyses

Statistical analyses were conducted using SPSS version 25 (IBM Corp.; Armonk, NY, USA). Data are presented as mean  $\pm$  standard deviation. Normality was analyzed using the Shapiro–Wilk normality test for all groups. The *F*-test was used to determine the homoscedasticity for all comparisons. All the groups were normally distributed ( $p > 0.05$ ). Two-tailed Welch’s *t*-test with Bonferroni correction or one-way analysis of variance (ANOVA), followed by Steel’s post hoc test against the control group, was used to analyze the differences;  $p < 0.05$  was considered to indicate a statistically significant difference ( $n = 3$ –4).

**Supplementary Materials:** The following supporting information can be downloaded at: <https://www.mdpi.com/article/10.3390/kinasesphosphatases1010003/s1>, Figure S1: Full membrane, Strong exposure, and Original for Figure 1B; Figure S2: Full membrane and Strong exposure for Figure 2A; Figure S3: Full membrane for Figure 3; Table S1: Primers.

**Author Contributions:** Conceptualization, S.T.; methodology, S.T. and T.K.; validation, S.T., Y.H. and T.K.; formal analysis, S.T., Y.H., M.S., K.F. and N.Y.; resources, S.T. and T.K.; data curation, S.T. and T.K.; writing—original draft preparation, S.T.; writing—review and editing, T.K.; visualization, S.T.; supervision, T.K.; project administration, S.T.; funding acquisition, S.T. All authors have read and agreed to the published version of the manuscript.

**Funding:** This research was funded by MEXT/JSPS KAKENHI Grant Number 16K08533, 19K06891, and the Takeda Science Foundation 2018 (to S. Tanaka).

**Institutional Review Board Statement:** All animal experiments were conducted in accordance with the Guidelines for the Care and Use of Laboratory Animals of the National Institute of Health, and were approved by the Ethics committee on Animal Experiments of Tokyo Metropolitan Institute of Medical Science (Tokyo, Japan; approval ID: approval ID: 22-27).

**Informed Consent Statement:** Not applicable.

**Data Availability Statement:** The datasets used and/or analyzed during the current study are available from the corresponding author upon reasonable request.

**Conflicts of Interest:** The authors declare no conflict of interest.

## References

1. Modi, V.; Dunbrack, R.L., Jr. A Structurally-Validated Multiple Sequence Alignment of 497 Human Protein Kinase Domains. *Sci. Rep.* **2019**, *9*, 19790. [[CrossRef](#)] [[PubMed](#)]
2. Ligos, J.M.; Gerwin, N.; Fernandez, P.; Gutierrez-Ramos, J.C.; Bernad, A. Cloning, expression analysis, and functional characterization of PKL12, a member of a new subfamily of ser/thr kinases. *Biochem. Biophys. Res. Commun.* **1998**, *249*, 380–384. [[CrossRef](#)] [[PubMed](#)]
3. Stairs, D.B.; Perry Gardner, H.; Ha, S.I.; Copeland, N.G.; Gilbert, D.J.; Jenkins, N.A.; Chodosh, L.A. Cloning and characterization of Krct, a member of a novel subfamily of serine/threonine kinases. *Hum. Mol. Genet.* **1998**, *7*, 2157–2166. [[CrossRef](#)] [[PubMed](#)]
4. Kurioka, K.; Nakagawa, K.; Denda, K.; Miyazawa, K.; Kitamura, N. Molecular cloning and characterization of a novel protein serine/threonine kinase highly expressed in mouse embryo. *Biochim. Biophys. Acta* **1998**, *1443*, 275–284. [[CrossRef](#)] [[PubMed](#)]
5. Berson, A.E.; Young, C.; Morrison, S.L.; Fujii, G.H.; Sheung, J.; Wu, B.; Bolen, J.B.; Burkhardt, A.L. Identification and characterization of a myristylated and palmitylated serine/threonine protein kinase. *Biochem. Biophys. Res. Commun.* **1999**, *259*, 533–538. [[CrossRef](#)]
6. Ohta, S.; Takeuchi, M.; Deguchi, M.; Tsuji, T.; Gahara, Y.; Nagata, K. A novel transcriptional factor with Ser/Thr kinase activity involved in the transforming growth factor (TGF)-beta signalling pathway. *Biochem. J.* **2000**, *350*, 395–404. [[CrossRef](#)]
7. Wang, J.; Ji, X.; Liu, J.; Zhang, X. Serine/Threonine Protein Kinase STK16. *Int. J. Mol. Sci.* **2019**, *20*, 1760. [[CrossRef](#)]
8. Guinea, B.; Ligos, J.M.; Lain de Lera, T.; Martin-Caballero, J.; Flores, J.; Gonzalez de la Pena, M.; Garcia-Castro, J.; Bernad, A. Nucleocytoplasmic shuttling of STK16 (PKL12), a Golgi-resident serine/threonine kinase involved in VEGF expression regulation. *Exp. Cell Res.* **2006**, *312*, 135–144. [[CrossRef](#)]

9. Ligos, J.M.; de Lera, T.L.; Hinderlich, S.; Guinea, B.; Sanchez, L.; Roca, R.; Valencia, A.; Bernad, A. Functional interaction between the Ser/Thr kinase PKL12 and N-acetylglucosamine kinase, a prominent enzyme implicated in the salvage pathway for GlcNAc recycling. *J. Biol. Chem.* **2002**, *277*, 6333–6343. [[CrossRef](#)]
10. Liu, J.; Yang, X.; Li, B.; Wang, J.; Wang, W.; Liu, J.; Liu, Q.; Zhang, X. STK16 regulates actin dynamics to control Golgi organization and cell cycle. *Sci. Rep.* **2017**, *7*, 44607. [[CrossRef](#)]
11. Sorrell, F.J.; Szklarz, M.; Abdul Azeez, K.R.; Elkins, J.M.; Knapp, S. Family-wide Structural Analysis of Human Numb-Associated Protein Kinases. *Structure* **2016**, *24*, 401–411. [[CrossRef](#)] [[PubMed](#)]
12. Eswaran, J.; Bernad, A.; Ligos, J.M.; Guinea, B.; Debreczeni, J.E.; Sobott, F.; Parker, S.A.; Najmanovich, R.; Turk, B.E.; Knapp, S. Structure of the human protein kinase MPSK1 reveals an atypical activation loop architecture. *Structure* **2008**, *16*, 115–124. [[CrossRef](#)] [[PubMed](#)]
13. Zhou, J.; Ma, S.; Wang, D.; Zeng, J.; Jiang, T. FreePSI: An alignment-free approach to estimating exon-inclusion ratios without a reference transcriptome. *Nucleic Acids Res.* **2018**, *46*, e11. [[CrossRef](#)] [[PubMed](#)]
14. Li, J.; Wang, Y.; Meng, X.; Liang, H. Modulation of transcriptional activity in brain lower grade glioma by alternative splicing. *PeerJ* **2018**, *6*, e4686. [[CrossRef](#)] [[PubMed](#)]
15. Lee, H.; Cho, S.J.; Moon, I.S. The non-canonical effect of N-acetyl-D-glucosamine kinase on the formation of neuronal dendrites. *Mol. Cells* **2014**, *37*, 248–256. [[CrossRef](#)] [[PubMed](#)]
16. Islam, M.A.; Sharif, S.R.; Lee, H.; Moon, I.S. N-Acetyl-D-Glucosamine Kinase Promotes the Axonal Growth of Developing Neurons. *Mol. Cells* **2015**, *38*, 876–885. [[CrossRef](#)] [[PubMed](#)]
17. Islam, M.A.; Sharif, S.R.; Lee, H.; Seog, D.H.; Moon, I.S. N-acetyl-D-glucosamine kinase interacts with dynein light-chain roadblock type 1 at Golgi outposts in neuronal dendritic branch points. *Exp. Mol. Med.* **2015**, *47*, e177. [[CrossRef](#)]
18. Butkinaree, C.; Park, K.; Hart, G.W. O-linked beta-N-acetylglucosamine (O-GlcNAc): Extensive crosstalk with phosphorylation to regulate signaling and transcription in response to nutrients and stress. *Biochim. Biophys. Acta* **2010**, *1800*, 96–106. [[CrossRef](#)]
19. Love, D.C.; Hanover, J.A. The hexosamine signaling pathway: Deciphering the “O-GlcNAc code”. *Sci. STKE Signal Transduct. Knowl. Environ.* **2005**, *2005*, re13. [[CrossRef](#)]
20. Hayakawa, K.; Sakamoto, Y.; Kanie, O.; Ohtake, A.; Daikoku, S.; Ito, Y.; Shiota, K. Reactivation of hyperglycemia-induced hypocretin (HCRT) gene silencing by N-acetyl-d-mannosamine in the orexin neurons derived from human iPS cells. *Epigenetics* **2017**, *12*, 764–778. [[CrossRef](#)]
21. Hayakawa, K.; Hirokawa, M.; Tabei, Y.; Arai, D.; Tanaka, S.; Murakami, N.; Yagi, S.; Shiota, K. Epigenetic switching by the metabolism-sensing factors in the generation of orexin neurons from mouse embryonic stem cells. *J. Biol. Chem.* **2013**, *288*, 17099–17110. [[CrossRef](#)] [[PubMed](#)]
22. Hayakawa, K.; Ohgane, J.; Tanaka, S.; Yagi, S.; Shiota, K. Oocyte-specific linker histone H1foo is an epigenomic modulator that decondenses chromatin and impairs pluripotency. *Epigenetics* **2012**, *7*, 1029–1036. [[CrossRef](#)]
23. de Lecea, L.; Sutcliffe, J.G. The hypocretins and sleep. *FEBS J.* **2005**, *272*, 5675–5688. [[CrossRef](#)] [[PubMed](#)]
24. Sakurai, T. The neural circuit of orexin (hypocretin): Maintaining sleep and wakefulness. *Nat. Rev. Neurosci.* **2007**, *8*, 171–181. [[CrossRef](#)] [[PubMed](#)]
25. Saper, C.B.; Fuller, P.M.; Pedersen, N.P.; Lu, J.; Scammell, T.E. Sleep state switching. *Neuron* **2010**, *68*, 1023–1042. [[CrossRef](#)]
26. Oughtred, R.; Rust, J.; Chang, C.; Breitkreutz, B.J.; Stark, C.; Willems, A.; Boucher, L.; Leung, G.; Kolas, N.; Zhang, F.; et al. The BioGRID database: A comprehensive biomedical resource of curated protein, genetic, and chemical interactions. *Protein Sci. A Publ. Protein Soc.* **2021**, *30*, 187–200. [[CrossRef](#)] [[PubMed](#)]
27. Kasahara, K.; Kawakami, Y.; Kiyono, T.; Yonemura, S.; Kawamura, Y.; Era, S.; Matsuzaki, F.; Goshima, N.; Inagaki, M. Ubiquitin-proteasome system controls ciliogenesis at the initial step of axoneme extension. *Nat. Commun.* **2014**, *5*, 5081. [[CrossRef](#)]
28. Lecker, S.H.; Goldberg, A.L.; Mitch, W.E. Protein degradation by the ubiquitin-proteasome pathway in normal and disease states. *J. Am. Soc. Nephrol. JASN* **2006**, *17*, 1807–1819. [[CrossRef](#)]
29. Fan, W.H.; Hou, Y.; Meng, F.K.; Wang, X.F.; Luo, Y.N.; Ge, P.F. Proteasome inhibitor MG-132 induces C6 glioma cell apoptosis via oxidative stress. *Acta Pharmacol. Sin.* **2011**, *32*, 619–625. [[CrossRef](#)]
30. Li, W.; Ye, Y. Polyubiquitin chains: Functions, structures, and mechanisms. *Cell. Mol. Life Sci. CMLS* **2008**, *65*, 2397–2406. [[CrossRef](#)]
31. Pickart, C.M. Mechanisms underlying ubiquitination. *Annu. Rev. Biochem.* **2001**, *70*, 503–533. [[CrossRef](#)] [[PubMed](#)]
32. Weissman, A.M. Themes and variations on ubiquitylation. *Nat. Reviews. Mol. Cell Biol.* **2001**, *2*, 169–178. [[CrossRef](#)] [[PubMed](#)]
33. Huttlin, E.L.; Bruckner, R.J.; Navarrete-Perea, J.; Cannon, J.R.; Baltier, K.; Gebreab, F.; Gygi, M.P.; Thornock, A.; Zarraga, G.; Tam, S.; et al. Dual proteome-scale networks reveal cell-specific remodeling of the human interactome. *Cell* **2021**, *184*, 3022–3040+e28. [[CrossRef](#)]
34. Young, B.D.; Sha, J.; Vashisht, A.A.; Wohlschlegel, J.A. Human Multisubunit E3 Ubiquitin Ligase Required for Heterotrimeric G-Protein beta-Subunit Ubiquitination and Downstream Signaling. *J. Proteome Res.* **2021**, *20*, 4318–4330. [[CrossRef](#)]
35. Prakash, S.; Tian, L.; Ratliff, K.S.; Lehotzky, R.E.; Matouschek, A. An unstructured initiation site is required for efficient proteasome-mediated degradation. *Nat. Struct. Mol. Biol.* **2004**, *11*, 830–837. [[CrossRef](#)] [[PubMed](#)]
36. Beekman, J.M.; Vervoort, S.J.; Dekkers, F.; van Vessel, M.E.; Vendelbosch, S.; Brugulat-Panes, A.; van Loosdregt, J.; Braat, A.K.; Coffey, P.J. Syntenin-mediated regulation of Sox4 proteasomal degradation modulates transcriptional output. *Oncogene* **2012**, *31*, 2668–2679. [[CrossRef](#)] [[PubMed](#)]

37. Kikuma, K.; Li, X.; Perry, S.; Li, Q.; Goel, P.; Chen, C.; Kim, D.; Stavropoulos, N.; Dickman, D. Cul3 and insomnia are required for rapid ubiquitination of postsynaptic targets and retrograde homeostatic signaling. *Nat. Commun.* **2019**, *10*, 2998. [[CrossRef](#)]
38. Pfeiffenberger, C.; Allada, R. Cul3 and the BTB adaptor insomnia are key regulators of sleep homeostasis and a dopamine arousal pathway in *Drosophila*. *PLoS Genet.* **2012**, *8*, e1003003. [[CrossRef](#)]
39. Stavropoulos, N.; Young, M.W. insomnia and Cullin-3 regulate sleep and wakefulness in *Drosophila*. *Neuron* **2011**, *72*, 964–976. [[CrossRef](#)]
40. Ryu, K.Y.; Fujiki, N.; Kazantzis, M.; Garza, J.C.; Bouley, D.M.; Stahl, A.; Lu, X.Y.; Nishino, S.; Kopito, R.R. Loss of polyubiquitin gene Ubb leads to metabolic and sleep abnormalities in mice. *Neuropathol. Appl. Neurobiol.* **2010**, *36*, 285–299. [[CrossRef](#)]
41. Peng, W.; Wu, Z.; Song, K.; Zhang, S.; Li, Y.; Xu, M. Regulation of sleep homeostasis mediator adenosine by basal forebrain glutamatergic neurons. *Science* **2020**, *369*, eabb0556. [[CrossRef](#)]
42. Szymusiak, R.; McGinty, D. Hypothalamic regulation of sleep and arousal. *Ann. N.Y. Acad. Sci.* **2008**, *1129*, 275–286. [[CrossRef](#)] [[PubMed](#)]
43. Takahashi, M.; Tahara, Y. Timing of Food/Nutrient Intake and Its Health Benefits. *J. Nutr. Sci. Vitam.* **2022**, *68*, S2–S4. [[CrossRef](#)] [[PubMed](#)]
44. Lee, Y.; Field, J.M.; Sehgal, A. Circadian Rhythms, Disease and Chronotherapy. *J. Biol. Rhythm.* **2021**, *36*, 503–531. [[CrossRef](#)] [[PubMed](#)]
45. Wang, Z.; Ma, J.; Miyoshi, C.; Li, Y.; Sato, M.; Ogawa, Y.; Lou, T.; Ma, C.; Gao, X.; Lee, C.; et al. Quantitative phosphoproteomic analysis of the molecular substrates of sleep need. *Nature* **2018**, *558*, 435–439. [[CrossRef](#)] [[PubMed](#)]
46. Fink, C.C.; Meyer, T. Molecular mechanisms of CaMKII activation in neuronal plasticity. *Curr. Opin. Neurobiol.* **2002**, *12*, 293–299. [[CrossRef](#)]
47. Tone, D.; Ode, K.L.; Zhang, Q.; Fujishima, H.; Yamada, R.G.; Nagashima, Y.; Matsumoto, K.; Wen, Z.; Yoshida, S.Y.; Mitani, T.T.; et al. Distinct phosphorylation states of mammalian CaMKIIbeta control the induction and maintenance of sleep. *PLoS Biol.* **2022**, *20*, e3001813. [[CrossRef](#)]
48. Belfort, G.M.; Kandror, K.V. Cellugyrin and synaptogyrin facilitate targeting of synaptophysin to a ubiquitous synaptic vesicle-sized compartment in PC12 cells. *J. Biol. Chem.* **2003**, *278*, 47971–47978. [[CrossRef](#)]
49. Tanaka, S.; Honda, Y.; Honda, M.; Yamada, H.; Honda, K.; Kodama, T. Anti-Tribbles Pseudokinase 2 (TRIB2)-Immunization Modulates Hypocretin/Orexin Neuronal Functions. *Sleep* **2017**, *40*, zsw036. [[CrossRef](#)]
50. Tanaka, S.; Honda, Y.; Takaku, S.; Koike, T.; Oe, S.; Hirahara, Y.; Yoshida, T.; Takizawa, N.; Takamori, Y.; Kurokawa, K.; et al. Involvement of PLAGL1/ZAC1 in hypocretin/orexin transcription. *Int. J. Mol. Med.* **2019**, *43*, 2164–2176. [[CrossRef](#)]
51. Tanaka, S.; Kodama, T.; Nonaka, T.; Toyoda, H.; Arai, M.; Fukazawa, M.; Honda, Y.; Honda, M.; Mignot, E. Transcriptional regulation of the hypocretin/orexin gene by NR6A1. *Biochem. Biophys. Res. Commun.* **2010**, *403*, 178–183. [[CrossRef](#)] [[PubMed](#)]
52. Terao, A.; Wisor, J.P.; Peyron, C.; Apte-Deshpande, A.; Wurts, S.W.; Edgar, D.M.; Kilduff, T.S. Gene expression in the rat brain during sleep deprivation and recovery sleep: An Affymetrix GeneChip study. *Neuroscience* **2006**, *137*, 593–605. [[CrossRef](#)] [[PubMed](#)]
53. Takizawa, N.; Tanaka, S.; Oe, S.; Koike, T.; Matsuda, T.; Yamada, H. Hypothalamohypophysial system in rats with autotransplantation of the adrenal cortex. *Mol. Med. Rep.* **2017**, *15*, 3215–3221. [[CrossRef](#)] [[PubMed](#)]

**Disclaimer/Publisher’s Note:** The statements, opinions and data contained in all publications are solely those of the individual author(s) and contributor(s) and not of MDPI and/or the editor(s). MDPI and/or the editor(s) disclaim responsibility for any injury to people or property resulting from any ideas, methods, instructions or products referred to in the content.